

A Vision System for Inspection of Ball Bonds in Integrated Circuits *

Alireza Khotanzad, Haimanti Banerjee, and Mandyam Srinath
Image Processing and Analysis Laboratory
Electrical Engineering Department
Southern Methodist University
Dallas, Texas 75275

Abstract

This paper describes a vision system for automatic inspection of the connecting part of the wire bond of an IC where the wire connects to the bond pad on the chip. It considers a popular type of such bonds known as "ball bond". Using two-dimensional images taken from the top of the IC wafer, the system determines several geometric measures which are important in determining the quality of the bond. These measures include the boundary, length of major and minor axes of the best fitting ellipse and the center. The process utilizes automatic thresholding, morphological operations and geometric moments of the image. Success of the method is demonstrated through experimental studies on actual bonds.

1: Introduction

One of the critical procedures in semiconductor device manufacturing is making the electrical interconnections inside the device's protective enclosure. These fine leads connect active microelectronic circuit chips to sturdy electrodes which ultimately mate with external electrical components as shown in Fig. 1. One of the problems in increasing reliability in the manufacture of integrated circuit devices is that of inspection of such bonding. Although vision-based inspection systems have been integrated in many stages of IC manufacturing, there has been little attempt to do so for wire bond inspection. At present, no commercial system is available for this task and such inspection and quality control is done off-line and frequently on a sample basis by human operators. In addition to being expensive and time-consuming, the results of such testing are also somewhat subjective due to factors such as fatigue and limitations of

human visual consistency. An automated system, on the other hand, leads to increased consistency and reliability of the inspection process. Further, the continuing increase in packing density of VLSI circuits requires that the inspection process be completely automated. For such a scheme to be feasible, the algorithms and techniques used in the inspection process must be implementable on workstations of reasonable cost.

This paper presents a description of an automated system for the inspection of the quality of the ball bond which is the connecting point between the pad and the wire to the lead finger. The location of the ball bond on the bond pad and its shape are important in determining the overall quality of the bond. In general, the bond should be centered in the middle of the pad and in many instances should be as close to circular in shape as possible. Here, we describe a system to automatically determine the location of the ball bond from two-dimensional images taken from the top of IC wafer, and to extract geometric measures describing its shape. These measures are obtained from the best fitting ellipse to the ball bond. The system was developed in collaboration with Process Automation Center of Texas Instruments, Inc.

The images to be processed by this system are taken from the top of the IC. It is assumed that the field of view of the image is set such that a small window around an individual ball bond is captured. Therefore, the contents of the image are the ball bond, part of the connecting wire, some of the bond pad and part of the chip itself. This is a very practical assumption since accurate alignment of the bonding mechanism with respect to the chip has to take place before bonding can be performed. This information can be made available to such a vision system and the system can use it to capture the described images of the individual bonds.

* This work was supported in part by a Grant from Texas Instrument, Inc.

Another factor to be noted is that the images are obtained in a controllable environment. The optics used to illuminate the scene can be easily adjusted for a particular device. Hence the quality of the obtained picture is good. The images we consider here are typical of those one can get with a simple optics set up.

As mentioned before, there are many commercially available vision systems for different stages of IC manufacturing. However none is available for wire bond inspection. A major factor in putting such little effort in this area is the fact that the system has to deal with a variety of bond shapes. In addition, unlike other routine inspection tasks, there is no standard pattern or template to look for or compare against.

At this point, it is appropriate to mention a few other vision systems which consider some aspects of bonds/bond pads. One such system is developed for wafer probing. Immediately after fabrication, IC's should be electrically tested to check for continuity. This is done by placing a sharp edged probe on bonding pads. In [2] a vision system is developed which determines the orientation of the wafer and the distance of the probe from the surface of the bond pad. This information is then used to control the automatic lowering of the probe until it touches the target pad without scratching its surface. This system uses a Hough transform technique along with edge information to locate the pads.

A related work considers the next stage after wafer probing. At this stage, the bond pads must be inspected to check for any defects caused by probing. A system discussed in [1] is developed for this task. This system checks for the following: (a) probe marks should not exceed the pad boundary, (b) scratches on the pad must not exceed 50 percent of the pad width and (c) the probe marks must not exceed 25 percent of the bond pad area. The algorithm extracts probe marks using a local thresholding method. It also identifies the protrusions of the marks beyond the pad boundary using morphological filtering.

The stages of our algorithm are: edge enhancement, automatic binarization, ball bond segmentation and detection of its boundary, neck (joining point of the wire and ball bond) identification and ellipse fitting using geometrical moments. The details of these steps along with the results of experimental studies using actual ball bond images are provided in the subsequent sections.

2: Description of the data base

The images used in this study were supplied by Texas Instruments, Inc. Twenty pictures of entire integrated circuits of different devices were given to us. A typical image is shown in Fig. 2. A 50×50 pixel wide window is set around each pad to separate the pad and its corresponding bond from the entire picture. The side view of a typical ball bond with wire is shown in Fig. 3. A data base consisting of all such sub-images that could be extracted from the twenty supplied images was constructed. Fig. 4 shows 28 images of this data base. Four images out of these 28 are shown in the first column of Fig. 5. In the rest of our discussion these four images will be used to illustrate different stages of the algorithm and only final results are shown for the rest of the images.

3: Edge enhancement

No illumination adjustment was attempted to improve the quality of the pictures which are obtained from a CCD camera. Therefore, the images in the data base are of various quality ranging from good to poor. In the present context, good quality image implies that there is a high contrast between the bond and the bond pad. For such images, the bond contour can be extracted by thresholding the image. However, in the case of images with low contrast between the bond and the bond pad, thresholding causes part of the edge to be lost. For this reason, prior to the thresholding operation, an edge-enhancement operation is performed on the original image using a Sobel operator [4] followed by mapping the absolute values within 0 and 255 linearly from 0 to 255 and any value beyond 255 as 255. The enhanced images of Fig. 5(a) are shown in Fig. 5(b). Note that for the bond in the third row, edge enhancement brings out the edge between the bond and the bond pad on the left side, which is not apparent in the original image.

4: Automatic binarization

The edge-enhanced image is binarized by comparing the pixel intensities to a threshold value. Those pixels belonging to the bond ball and its connecting wire are assigned as black while the background pixels are painted white. The appropriate threshold is decided automatically by analyzing the histogram of the image. Several thresholding techniques available in the literature were used on the images. It was found that the best results were obtained using an optimal

thresholding technique suggested by Otsu [5]. In this technique, the optimal threshold, T , is selected by maximizing a measure of separability, $J_o(T)$, between the two classes of pixels, where

$$J_o(T) = \frac{N_1(T)N_2(T)[\mu_1(T) - \mu_2(T)]^2}{[N_1(T) + N_2(T)]}$$

where $N_i(T)$, $i = 1, 2$ represents the number of pixels belonging to the i th class and $\mu_i(T)$, $i = 1, 2$, is the corresponding sample mean. The optimum threshold is chosen to be the one that maximizes $J_o(T)$. It can be analytically shown that such a choice minimizes intra-class variations while maximizing inter-class separation between two populations. The results of binarization of the edge-enhanced images of Fig. 5(b) are shown in Fig. 5(c).

5: Ball bond segmentation

The next step in the process is aimed at isolating the part of the image corresponding to the bond. To do so, one must identify and remove the part corresponding to the connecting wire so as to obtain a closed contour (blob) of the ball bond alone. Two different methods are developed for this task.

In the first method, the approximate center of the ball bond is first determined using morphological erosion operation. Then, through radial scanning from this center, the ball bond contour is found and the gap corresponding to neck is identified.

The second approach is purely morphological and relies on a series of erosion and dilation operations to compute the ball bond blob.

5.1: Center computation and radial scanning method

The first step in this procedure is to use a series of morphological operations on the binary image in order to determine the approximate center of the bond. This procedure is based on the fact that the ball bond is a large circular silhouette in the image. The procedure is to iteratively erode the bond silhouette with a small disk characterized by a 3×3 kernel:

$$\begin{matrix} 1 & 1 & 1 \\ 1 & 1 & 1 \\ 1 & 1 & 1 \end{matrix}$$

In each iteration the black pixels are eroded (i.e. changed to white) from the remaining border of the bond. This is done by changing a black pixel (0) to a white (1) pixel, if any of its neighbors in an eight connected neighborhood is white. The iterations are continued until a point is reached where another erosion will cause all the black pixels to disappear. At that stage, either a single black pixel or a small group of black pixels will remain. In the former case, the remaining pixel is taken as the center. In the latter case, the geometric centroid of the remaining group of pixels is computed to find the center. The coordinate of the centroid is computed by finding the average of the coordinates of the remaining pixels.

This process of extracting the bond center is illustrated in Fig. 6. As can be seen from the figure, for this image, eleven iterations of erosion are needed to obtain the center. At the final step only one pixel remains for this image. This is the approximate location of the center for this particular image. Fig. 7 shows another example where more than one pixel remain in the final iteration. After this stage any further iteration will make all the pixels vanish as shown in Fig. 7. In this case the centroid is found by computing the average of the coordinates of the black pixels left before the last erosion. The computed centers of the bonds in Fig. 5(c) are shown in Fig. 5(d).

In the next stage, the computed center is used to extract the ball-bond boundary. The image is scanned at one degree intervals along each radial direction from the center for the first white pixel, which is then assumed to be a point on the ball boundary. All other pixels in the same radial direction beyond the first white pixel are removed. Figure 5(e) shows the result of this operation. However, as can be seen in Fig. 5(e), with some images, some background pixels which do not constitute part of the ball boundary are also retained. Typically, these extraneous pixels are not continuous with the ball boundary and correspond to those pixels which can be scanned along a radial direction from the center through a gap in the boundary. Distance-wise these points are all further from the center than typical radius of the bond ball. This property is used to eliminate these undesirable pixels. Thus the main objective of the next step is to mark the pixels which are far beyond the average distance between the center and the bond contour. This is done by first computing the mean, μ_r , and standard deviation, σ_r , of the radial distances from the center to the boundary pixels obtained in the previous step and retaining those pixels whose distance to the center, r , satisfy

$$r \leq \mu_r + \alpha \sigma_r$$

and marking the rest as potential candidates for elimination. In other words, if a detected boundary pixel has an unusually far distance from the center, it is likely that it would not be on the boundary. In this work $\alpha = 0.7$ is used. However, the procedure is not very sensitive to this value since further checks will eliminate problems that might arise due to the choice for α . Fig. 5(f) shows the retained pixels for the image in Fig. 5(e). As can be seen, this causes some of the good but irregularly shaped (in terms of distance from the center) boundary pixels to be marked as well. Thus more checks need to be made before elimination of the marked pixels as undesired.

The next test involves examining the spatial location and connectedness of the marked pixels. If such a pixel is isolated, i.e. has no other black pixel in its 8-connected neighborhood, then it is eliminated. However, if it has one or several neighbors, then it will be part of a connected component. The start and the end points of this component are then determined. If one or both of them are neighbors of any one of the retained pixels, this connected component is assumed to be part of the good boundary and it is therefore not eliminated. Otherwise, it is a connected component in the background and is eliminated. Fig. 5(g) shows this stage of the operation. Note that some of the good boundary pixels which were not retained in Fig. 5(f) reappear as a result of this series of tests as shown in Fig. 5(g).

In the next stage, all the gaps in the border are determined and the gap corresponding to the neck is identified. This is done by marking the mid-point of each gap and examining the pixels along the radial direction from the center to the mid-point in the binary image (Fig. 5(c)). The neck gap will be the one which has the largest number of connected black pixels in that direction. Knowledge about the location of the neck is important since it can provide information about the position of the connecting wires.

The procedure for fitting an ellipse to the bond requires a blob (closed contour). To obtain a closed boundary for the bond, any gap including the neck gap is filled out by interpolations. The slope of the line joining the start and end points of the gap is computed. Beginning with the starting point of the gap, the 8-connected pixel whose slope is the closest to the slope computed above is found and marked. This process is continued until the end point of the gap is reached. The process is illustrated in Fig. 8. Points A and B are starting and end points of a neck gap. The slope of the gap, AB is determined first. The slope Aa

is the closest one to the slope of AB. Therefore the pixel a is selected. Thus the path AabcdeB is obtained through the same procedure.

The resulting closed boundary for the images in Fig. 5(g) are shown in Fig. 5(h). Fig. 9 shows the detected contours for all the other images.

5.2: Successive erosion and dilation method

An alternative approach to extraction of the ball bond contour through morphological operation is described in this section. The motivation behind this second approach is the high computational demand of the radial scanning procedure which makes the algorithm rather slow. In this approach, the ball bond is segmented through repetitive erosions and dilations of the image. It does not require radial scanning and as such can be performed faster than the previous method.

Again the foundation of the method is based on the fact that the largest circular shape in the image is that of the ball bond and the neck portion has a smaller width compared to the main body of the bond. Thus, if one erodes the silhouette in the same manner discussed in the previous section, the neck and the connecting wire along with other extraneous pixels will disappear after a few iterations while some part of the main body of the bond will still remain (Fig. 10 (e) using 6 erosions). After this stage is reached, the obtained silhouette is dilated $m+1$ times where m is the number of erosions performed (Fig. 10 (f)). Dilation by a circular disc is the reverse operation of erosion, i.e. a white (1) pixel is changed to a black (0) pixel if any of its eight neighbor in an 8-connected neighborhood is black. Since one additional dilation is performed, the obtained silhouette will be slightly larger than the original one. In addition, the shape will also be different from the original silhouette. Now, this m -eroded, $m+1$ -dilated blob is used as a mask to determine the ball bond blob in the original binary image. This is done by performing a logical AND operation between the two images (Fig. 10 (g)). The final result is a blob from which the wire is disconnected. The neck region gap is also connected eliminating the need for another procedure to close it.

6: Determination of the best fitting ellipse

As stated earlier, the quality of the bond is determined by the location of the bond on the bond pad and its shape. While the center of the bond gives the location of the bond on the bond pad, measures of

circularity can be used to determine how close its shape is to being a circle.

A set of such measures can be obtained by determining the best-fitting ellipse to the extracted ball bond blob (i.e. the ball contour and its interior). Using analytic geometry techniques, it is shown in [6] that the parameters of the best-fitting ellipse, namely the lengths of the major and minor axes and its orientation can be computed from the following second-order geometric (spatial) moments of the silhouette (blob):

Let the binary image be $M \times N$

Second order row moment:

$$\mu_{rr} = \sum_{r=1}^M (r - \bar{r})^2 / A$$

Second order column moment:

$$\mu_{cc} = \sum_{c=1}^N (c - \bar{c})^2 / A$$

Second order mixed moment:

$$\mu_{rc} = \sum_{c=1}^N \sum_{r=1}^M (r - \bar{r})(c - \bar{c}) / A$$

where A is the number of silhouette pixels, (r,c) is the location of a silhouette pixel and (\bar{r}, \bar{c}) is the location of the centroid.

Several cases need to be considered :

a) $\mu_{rc} = 0$

(a.1.) $\mu_{rr} > \mu_{cc}$: major axis is of length $4 \mu_{rr}^{1/2}$ and oriented at an angle of -90° counterclockwise from column axis; minor axis is of length $4 \mu_{cc}^{1/2}$ and oriented at 0° from the column axis.

(a.2.) $\mu_{rr} \leq \mu_{cc}$: major axis is of length $4 \mu_{cc}^{1/2}$ and its orientation is at 0° from the column axis; minor axis is of length $4 \mu_{rr}^{1/2}$ and is oriented at -90° counterclockwise from the column axis.

b) $\mu_{rc} \neq 0$

(b.1.) $\mu_{rr} > \mu_{cc}$: the length of the major axis is

$$[8(\mu_{rr} + \mu_{cc} + ((\mu_{rr} - \mu_{cc})^2 + 4\mu_{rc}^2)^{1/2})]^{1/2}$$

and its orientation is at an angle

$$\phi = \tan^{-1} \frac{\mu_{rr} - \mu_{cc} + \sqrt{(\mu_{rr} - \mu_{cc})^2 + 4\mu_{rc}^2}}{-2\mu_{rc}}$$

The minor axis is at 90° counterclockwise with the major axis and the length is

$$[8(\mu_{rr} + \mu_{cc} - ((\mu_{rr} - \mu_{cc})^2 + 4\mu_{rc}^2)^{1/2})]^{1/2}$$

(b.2.) $\mu_{rr} \leq \mu_{cc}$: the major axis is of length

$$[8(\mu_{rr} + \mu_{cc} + ((\mu_{rr} - \mu_{cc})^2 + 4\mu_{rc}^2)^{1/2})]^{1/2}$$

at an angle

$$\phi = \tan^{-1} \frac{-2\mu_{rc}}{\mu_{cc} - \mu_{rr} + \sqrt{(\mu_{cc} - \mu_{rr})^2 + 4\mu_{rc}^2}}$$

The minor axis is at 90° counterclockwise with the major axis and the length is

$$[8(\mu_{rr} + \mu_{cc} - ((\mu_{rr} - \mu_{cc})^2 + 4\mu_{rc}^2)^{1/2})]^{1/2}$$

An image of the best fitting ellipse is generated based on the major axis, the minor axis and the orientation computed as above. Figs. 5(i) and 10(h) illustrates the results superimposed on the original images using the first and second segmentation methods respectively. Fig.11 and Fig. 12 show the same for all the other images.

A measure of circularity of the ball contour can be obtained as the ratio of the major axis to minor axis, which for a circle should be equal to unity. Table 1 lists this measure for ellipses of Figs 11 and 12 obtained with the two different segmentation methods. The closer this measure is to one, the more circular the bond is. Note that these measures correlate very well with visual appearance of the bonds.

7: Implementation

Both of the segmentation algorithms were implemented in Texas Instrument's vision system. The system has dedicated hardware for operations such as morphological erosion and dilation. The total execution time taken from image acquisition to the

determination of shape parameters for a single bond was noted to be around 1 sec using radial scanning method. Most of the time was taken by the border extraction using radial scanning method. The execution time for the second algorithm using morphological operations is 380 milliseconds since all the stages of the algorithm take advantage of dedicated hardware.

8: Conclusions

A method for computing some important geometrical measures for ball bonds is developed. These measures which are used in inspection of such bonds are obtained from parameters of the best fitting ellipses. The procedure is fully automatic and no manual adjustment of any parameter is required. The success of the approach was demonstrated by applying it to several images of ball bonds. The approach is computationally inexpensive and practical.

9: Acknowledgments

The authors acknowledge several useful discussions with Dr. Yee-Hsun U, Dr. David Ho and Bob Clunn, all with Process Automation Center, Texas Instruments, Inc., Dallas, Texas.

References

1. M. Ahmed, C. E. Cole, R. C. Jain, A. R. Rao, "INSPAD: A System for Automatic Bond Pad Inspection", *IEEE Trans. Semiconductor Manufacturing*, pp. 145-147, Aug., 1990.
2. R. V. Dantu, N. J. Dimopoulos, R. V. Patel, A. J. Al-Khalili, "Micromanipulator Vision for Wafer Probing", *IEEE Trans. Semiconductor Manufacturing*, pp. 114-117, Aug., 1989.
3. B. L. Gehman, "Bonding Wire Microelectronic Interconnections", *IEEE Trans. Comp., Hybrid and Manufacturing Technology*, pp. 375-383, Sept., 1980.
4. R. C. Gonzalez and P. Wintz, *Digital Image Processing*, Addison-Wesley Publishing Co. Inc., 1987.
5. N. Otsu, "A Threshold Selection Method from Gray Level Histograms", *IEEE Trans. Systems, Man, and Cybernetics*, Vol. SMC-9, pp. 62-66, 1979.
6. R. M. Haralick and L. G. Shapiro, *Computer and Robot Vision*, Addison-Wesley Publishing Co. Inc., pp 639-658, 1992.

Table 1. Shape measures obtained from parameters of the Best Fitting Ellipse. Bond numbers refer to images of Fig. 4 number from left to right, bottom to top. Length measures are in pixels.

Bond No.	First Segmentation Method			Second Segmentation Method		
	Length	Length	Major	Length	Length	Major
	Major Axis	Minor Axis	Minor	Major Axis	Minor Axis	Minor
1	47.87	43.52	1.09	34.05	31.01	1.10
2	47.21	44.57	1.06	34.29	31.21	1.10
3	48.43	43.93	1.10	37.14	30.47	1.22
4	46.49	43.86	1.06	35.24	30.53	1.15
5	48.93	43.78	1.11	37.25	29.08	1.28
6	47.19	41.59	1.13	33.58	30.66	1.09
7	44.79	37.48	1.20	31.59	26.26	1.20
8	40.95	39.67	1.03	28.75	26.62	1.08
9	45.60	39.20	1.16	33.37	27.18	1.23
10	43.48	38.18	1.14	31.47	25.82	1.22
11	42.34	36.58	1.15	32.61	24.44	1.33
12	41.32	38.37	1.08	28.62	26.54	1.08
13	44.60	41.45	1.08	30.5	29.10	1.05
14	45.43	40.18	1.13	31.63	28.05	1.28
15	40.48	38.34	1.05	28.23	26.40	1.07
16	43.46	39.03	1.11	30.95	27.40	1.13
17	41.91	37.10	1.13	29.04	25.49	1.14
18	44.57	38.74	1.15	32.25	26.15	1.23
19	47.30	39.41	1.20	34.07	27.60	1.23
20	44.74	39.57	1.13	33.84	26.64	1.27
21	44.43	37.08	1.20	30.39	26.90	1.23
22	45.99	37.20	1.24	31.19	27.31	1.14
23	44.34	41.34	1.07	32.25	27.72	1.16
24	46.85	39.86	1.18	34.85	28.42	1.23
25	47.81	40.62	1.18	36.87	31.33	1.15
26	45.37	42.14	1.08	31.92	27.67	1.15
27	49.91	39.28	1.27	35.23	27.30	1.29
28	42.72	39.63	1.08	29.30	28.46	1.03

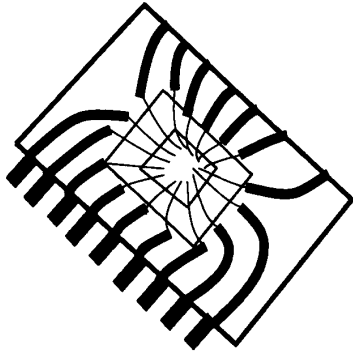


Fig. 1 Schematic of an Integrated Circuit showing the wire bonds.

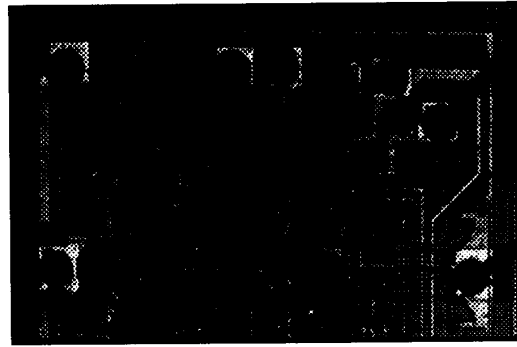


Fig. 2 A typical image of an Integrated Circuit. Wire bonds are the dark regions.

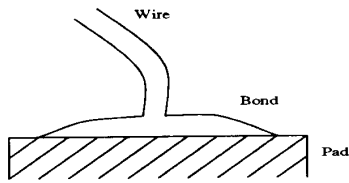


Fig. 3 Sideview of a typical ball bond

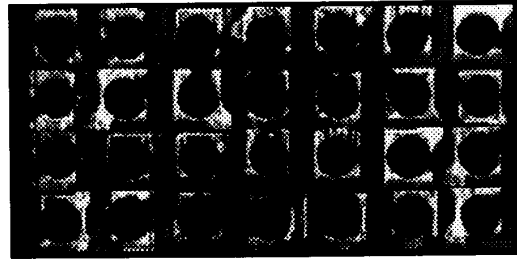


Fig. 4 Images of the ball bonds in the data base

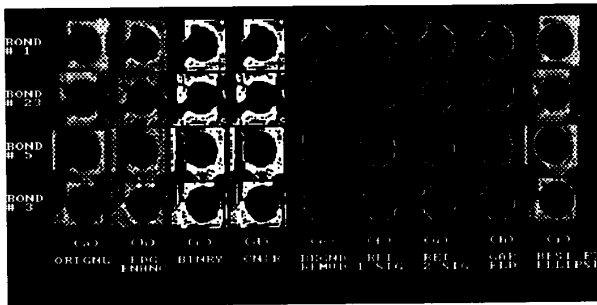


Fig. 5 Different stages of the algorithm using radial scanning method.

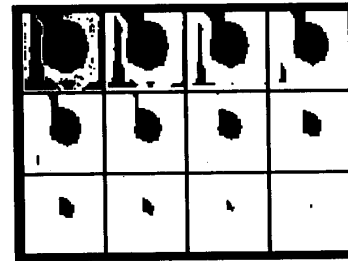


Fig. 6 Process of computing a bond center.

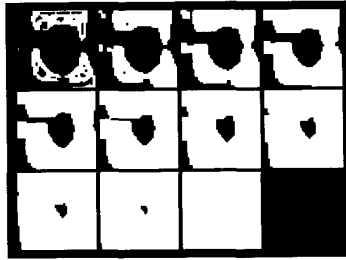


Fig. 7 Center finding process(more than one pixel at final iteration).

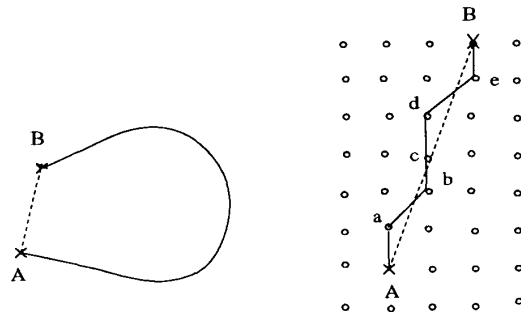


Fig. 8 Illustration of the gap filling procedure.

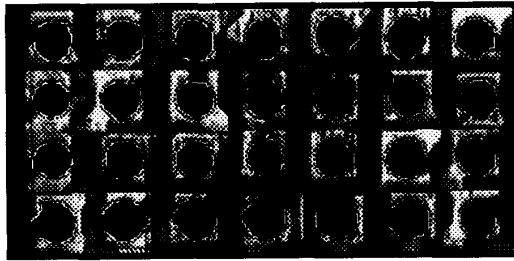


Fig. 9 Extracted ball bond boundary superimposed on original image.

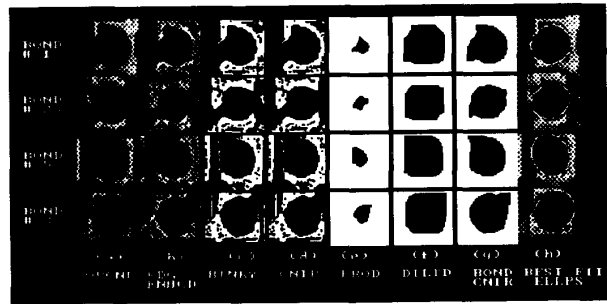


Fig. 10 Different stages of algorithm using successive erosion and dilation method for segmentation.

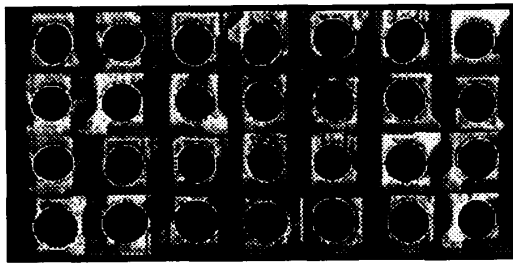


Fig. 11 Computed best fitting ellipse superimposed on original image using radial scanning method for segmentation.

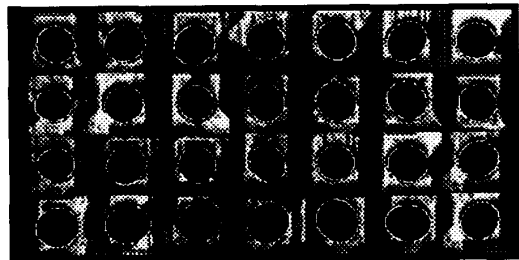


Fig. 12 Computed best fitting ellipse superimposed on original image using successive erosion and dilation method for segmentation.